Am J Physiol Gastrointest Liver Physiol 301: G498–G507, 2011.
First published June 16, 2011; doi:10.1152/ajpgi.00164.2011.

Myosin Va plays a key role in nitrergic neurotransmission by transporting nNOSα to enteric varicosity membrane

Arun Chaudhury, Xue-Dao He, and Raj K. Goyal

Center for Swallowing & Motility Disorders, VA Boston HealthCare System and Harvard Medical School, Boston, Massachusetts

Submitted 27 April 2011; accepted in final form 15 June 2011

Chaudhury A, He XD, Goyal RK. Myosin Va plays a key role in nitrergic neurotransmission by transporting nNOSα to enteric varicosity membrane. *Am J Physiol Gastrointest Liver Physiol* 301: G498–G507, 2011. First published June 16, 2011; doi:10.1152/ajpgi.00164.2011.—Nitrergic neurotransmission at the smooth muscle neuromuscular junctions requires nitric oxide (NO) release that is dependent on the transport and docking of neuronal NO synthase (nNOS) α to the membrane of nerve terminals. However, the mechanism of translocation of nNOSα in actin-rich varicosities is unknown. We report here that the processive motor protein myosin Va is necessary for nitrergic neurotransmission. In wild-type mice, nNOSα-stained enteric varicosities colocalized with myosin Va and its tail constituent light chain 8 (LC8). In situ proximity ligation assay showed close association among nNOSα, myosin Va, and LC8. nNOSα was associated with varicosity membrane. Varicosities showed nitric oxide production upon stimulation with KCl. Intracellular microelectrode studies showed nitrergic IJP and smooth muscle hyperpolarizing responses to NO donor diethylenetriamine-NO (DNO). In contrast, enteric varicosities from myosin Va-deficient DBA (for dilute, brown, non-agouti) mice showed near absence of myosin Va but normal nNOSα and LC8. Membrane-bound nNOSα was not detectable, and the varicosities showed reduced NO production. Intracellular recordings in DBA mice showed reduced nitrergic IJPs but normal hyperpolarizing response to DNO. The nitrergic slow IJP was 9.1 ± 0.7 mV in the wild-type controls and 3.4 ± 0.3 mV in the DBA mice ($P < 0.0001$). Deficiency of myosin Va resulted in loss of nitrergic neuromuscular neurotransmission despite normal presence of nNOSα in the varicosities. These studies reveal the critical importance of myosin Va in nitrergic neurotransmission by facilitating transport of nNOSα to the varicosity membrane.

DBA mice; LC8; enteric nerves; nitrergic inhibitory junction potential; myosin Va; active nNOS; inactive nNOS

NEURONAL NO SYNTHASE (nNOS) α-derived NO serves as both an anterograde and a retrograde neurotransmitter. Although it serves as a retrograde synaptic neurotransmitter at the glutamatergic synapses of central neurons (12), NO functions as an anterograde inhibitory neurotransmitter at smooth muscle neuromuscular junctions, particularly those in the gut (6, 22). NO is produced upon de novo synthesis from nNOSα (35). Studies on isolated nitrergic enteric nerve terminals have shown that nNOSα may exist as catalytically active and catalytically inactive forms, based on its ability to produce NO on exposure to calcium and calmodulin (7, 25, 30).

Catalytically active nNOSα should be localized to sites that facilitate genesis of NO (39). These sites are primarily characterized by proximity to a source of high Ca^{2+} and proteins such as CamKIIα and phosphatases that allosterically regulate the activity of nNOSα. These sites include plasma membranes and membranes of intracellular organelles (25). At the excitatory synapses of the CNS, active nNOSα is localized at the postsynaptic dendritic spines in immediate vicinity of PSD95 in the postsynaptic density, which assembles NMDA receptors that function as calcium channels (4). A related splice variant of nNOSα, nNOSμ, which is predominantly present in skeletal muscle cells, also preferentially localizes to plasma membranes (4).

In the enteric motor nerve terminals, catalytically active nNOSα associates with the cytoplasmic aspect of the varicosity membrane by binding to PSD95 via its PDZ binding domains (8). PSD95 is anchored to the membrane by palmitoylation where PSD95 may assemble calcium channels and other enzymes and proteins that may regulate the activity of nNOSα (7).

Catalytically inactive pool of nNOS is cytosolic in location in the enteric motor nerve terminals (8, 30). nNOS associates with several cytosolic adaptor proteins including dynein light chain 8 (LC8 or DLC8) (19, 31). LC8 has been reported to bind to catalytically inactive nNOS and may be involved in the storage and intravaricosity transport of nNOSα (8, 31).

The subcellular translocation of nNOSα to the site of its action requires nNOSα to be transported from the inactive cytosolic pool to the active pool at the plasma membrane. However, the mechanism of subcellular translocation of nNOSα is not well understood. Translocation of nNOSα may be passive in nature, for example, occurring by simple diffusion by Brownian motion. However, several studies have shown nNOSα translocation to be actively regulated. For example, in PC12 cells, translocation of nNOSα to the plasma membrane during active neurotransmission is stimulated by signaling molecules, including glutamate via NMDA receptor (1), pituitary adenylate cyclase-activating polypeptide (PACAP) via PACAP 1 receptor stimulation (21), and ATP via P2X and P2Y receptors involving protein kinase C (26).

These observations strongly suggest that the intracellular movement of nNOSα is highly regulated and fine tuned in enteric motor nerve terminals according to the needs of nitrergic neurotransmission. However, the molecular motors involved in the membrane targeting of nNOSα in the nitrergic enteric varicosities are not known. It has been suggested that LC8 may be involved in the transport of nNOSα in neuronal cells, including enteric motor terminals (8, 18, 31). LC8 is the light chain of the motor protein dynein as well as the actin-based motor myosin Va (2, 3, 9). Thus LC8 may serve as an adaptor protein for nNOS by binding to the myosin motor myosin Va. Whereas dynein is involved in microtubule-based retrograde axonal transport, myosin Va has been reported as a motor for short distance transport in the subcortical nerve

Address for reprint requests and other correspondence: R. K. Goyal, VA Medical Ctr., 1400 VFW Pkwy., West Roxbury, MA 02132 (e-mail: raj_goyal@hms.harvard.edu).

varicosity regions (5). We hypothesized that myosin Va may be involved in the translocation of nNOSα to the plasma membrane and that deficiency of myosin Va may lead to loss of nitrergic neurotransmission.

Studies in myosin Va-deficient mice have revealed the important roles of myosin Va in the intracellular transport of organelles, vesicles, proteins, and mRNA (32). We thus hypothesized that myosin Va-deficient mice may provide information on the role of myosin Va in the transport of nNOS to the varicosity membrane and nitrergic neurotransmission. Genetic loss of myosin Va may be complete or incomplete. Mice with a complete deficiency of myosin Va due to deletion of the MYO5A gene (dilute-lethal mice) die in infancy (23). However, DBA (dilute, brown, non-agouti) mice, with a partial deficiency of myosin Va due to mutation of the MYO5A gene by a viral insertion, survive into adulthood (17). The most characteristic feature of DBA mice is their lightening of coat color due to impaired transport of melanosomes in melanocytes and hence the label as "dilute" mice. They also exhibit a variety of neurological disorders due to defective intracellular transport of cargoes such as neurotransmitter vesicles. Syndromes of genetic deficiency of myosin Va are seen in many animal species including humans (Griscelli syndrome type 1). Griscelli syndrome type 1 is characterized by premature silvering of hair and less well characterized neurological and neuromuscular disturbances (27). Gastrointestinal function in clinical syndromes of myosin Va deficiency has not been examined.

We used isolated enteric varicosities from WT mice and determined that the myosin Va present in these varicosities was closely associated with nNOSα. K^+-induced stimulation of varicosities caused in vitro NO production. Enteric varicosities from DBA mice were used to determine the effect of myosin Va deficiency. We performed comparative intracellular electrophysiological studies in gastric antral muscle strips to determine whether nitrergic inhibitory junction potentials were affected in the myosin Va-deficient DBA mice. Together, these studies show that myosin Va plays a key role in transporting nNOS to the varicosity membrane and in nitrergic neurotransmission. Without myosin Va, transport of nNOS to the varicosity membrane and nitrergic neurotransmission is lost.

MATERIALS AND METHODS

All experiments were preapproved by the Institutional Animal Care and Use Committee, VA Boston HealthCare System (VABHS).

Animals

Male wild-type (WT) C57BL/6J mice (4–6 wk) with solid black coat color served as controls. Male DBA/2J and DBA/1J mice were used as models of myosin Va deficiency. Most ancient of all inbred strains, DBA mice (formerly, dba) were raised at National Institutes of Health and Jackson Laboratories by intercrossing homozygous for the coat colors dilute (*d/Myo5a*), brown (*b/Tyrp1*), non-agouti (*a*). The substrains 1J and 2J both have similar mutations in MYO5A and have no apparent phenotypic differences. DBA/2J mice were used in the present experiments based on similarity of initial pilot data.

Preparation of Enteric Varicosities

Varicosities were obtained from sub-diaphragmatic portions of gut of WT and DBA mice. An initial low-speed centrifugation removed nuclear and muscle debris. An intermediate-speed centrifugation yielded a supernatant that was layered on 0.8/1.2 M sucrose cushion that principally enriches the nerve terminals. Microsomal components or pelleted mitochondrial fragments were not used in the analytical materials. These preparatory methods are based on standardized methods of synaptosomal preparations using gut tissues (30, 37). Furthermore, these samples were examined for PGP9.5 and synaptophysin for their nerve terminal identity. Gut tissues were pooled from 10 mice in each group in WT animals ($n = 30$ total mice) and 6 mice in DBA ($n = 18$ total mice). Triplicates of these homogenates were prepared in each group. Aliquots of varicosities stored at −80°C were always kept on ice before and during experiments, unless otherwise described. For imaging (immunolocalization, PLA, in vitro NO assays) and immunoblotting experiments, all six pools (three groups from WT and three groups from DBA) were used. Multiple wells from each of these groups were stained simultaneously for control experiments (omitting primary antibody, etc.). Quantitative data were obtained cumulatively from all groups in each experiment. Representative images depicting each experimental condition are shown in the figures.

Antibodies

These were the primary antibodies used: myosin Va [H-90 that detects AA981-1070 (lot no. F0707, rabbit) and S-14 that identifies a 12- to 20-peptide region in the region encoded by exon E in the tail region spanning AA 1,350–1,400 (lot no. B2108, goat); SantaCruz Biotech]; nNOSα (NH_2-terminal specific K-20, lot no. J1606, rabbit; Santa Cruz and COOH-terminal specific polyclonal antibody, lot no. 952416, goat; Abcam), LC8 (FL-89) (lot no. J1304, rabbit) (SantaCruz Biotech) and PGP9.5 (lot no. Z06440c, rabbit) (Enzo). Appropriate secondary antibodies conforming to the correct species were used [donkey anti-goat AlexaFluor594 (lot no. 714270) and goat anti-rabbit AlexaFluor 488 (lot no. 828814); Molecular Probes]. Secondary antibodies were chosen bound to fluorophores with widely separated emission spectra to avoid spectral bleed through during imaging. Varicosities stained with the two types of myosin antibodies used in the present study showed complete overlap of staining patterns (data not shown). Specificity of nNOS and LC8 primary antibodies were tested by running samples of positive controls in gels that identified bands corresponding to respective molecular weights.

Immunostaining of Varicosities

Glass-bottom microwell dishes (MatTek) were used to stain varicosities. Varicosity sample (5–10 μl) was added in the well, equilibrated for an hour in the cold with isotonic phosphate-buffered saline, bovine serum albumin, and 0.1% sodium borohydride, and stained in the dark. Antibiotics were added to prevent growth of microorganisms, especially because cocci can resemble the rounded-appearing varicosities. Washes between steps were done using a buffer composed of 10 mM TES [*N*-tris(hydroxymethyl)-methyl-2-aminoethanesulfonic acid] added to a standard Krebs-like solution. The samples were fixed and permeabilized in cold 3% methanol-paraformaldehyde for 20 min and then incubated with 30 mM NH_4Cl for 10 min. Incubation with the primary antibodies was performed by dilution of the antibody in PBS-BSA. Pilot experiments determined optimal primary antibody concentrations (usually 1:50 to 1:100). The secondary antibody was added at a 10-fold dilution to the primary and stained for an hour. Controls were performed for all antibody-based staining by omitting one or both primary antibodies.

Visualization of Stained Varicosities With Confocal Laser Microscope

Subcellular imaging was performed with an inverted Nikon microscope (ECLIPSE TE2000-U, Nikon) interfaced with a confocal system (Nikon C1) and Melles-Griot lasers carrying 488- and 595-nm lines (bandwidth 515/30 and 590/50). Varicosities were examined

with a ×20 or a ×100 objective fitted with DIC optics (NA 0.7–1.4). At first, plated varicosities were localized under brightfield illumination. After localizing a signal in a field of view, confirmation of signal distribution within the varicosities was performed by digital image zooming. Scans were obtained using least laser powers. Several random fields from multiple samples in each group were scanned to confirm results. Tiff files of raw images were used for quantitative image analyses with NIH freeware ImageJ (Bethesda, MD) (http://imagej.nih.gov/ij/download.html). Colocalization coefficients of overlap of fluorescent signals were quantitatively estimated.

In Situ Proximity Ligation Assay

Proximity ligation in situ assay (PLA) was used to examine protein-protein interactions in an intact cellular environment (20). For PLA, freshly plated varicosities were studied using the Duolink in situ PLA detection kit (Olink, Uppsala, Sweden) per the vendor's instructions. Cells were incubated with primary antibodies to detect interactions of myosin Va with nNOSα and LC8 and LC8 interactions with nNOSα. Either antibody was omitted in control experiments. Cells were labeled with species-specific Duolink PLA PLUS and MINUS probes in a humidified oven at 37°C. The secondary antibodies of PLA PLUS and MINUS probes, based on synthetic oligonucleotide tails, hybridize when primary antibodies in close proximity (i.e., <40-nm separation). The amplification end products showed up as red fluorescent spots during fluorescence imaging. Each of these red spots is representative of several interacting protein-protein molecules. Mounting was performed in an aqueous medium for imaging.

Quantitation of PLA Signals

Semiquantitative analysis of the stochastic PLA signal was performed. Wide dynamic range thresholding and segmentation of the PLA fluorescent signals were used to quantitate the number of fluorescent blobs using the "blob" tool in Lispix (version lx163), available from NIST (National Institutes of Standards and Technology, Bethesda, MD). Data were expressed as mean number of blobs per varicosity.

Western Blot for Varicosity Membrane Localization of nNOSα

Membrane samples were prepared by incubating varicosity samples in a hypotonic buffer of low ionic concentrations of sodium phosphate and magnesium sulfate. Boiled samples of WT and DBA whole varicosities and membranes were electrophoresed in a 4–20% polyacrylamide gel and probed for nNOSα using the NH_2-terminal-specific antibody. Signal localization/absence was confirmed by varying antibody dilutions and exposure times.

In Vitro NO Imaging of Enteric Varicosities

Plated varicosities were perfused with Krebs' solution replete with L-arginine and nitric oxide synthesizing cofactors like NAD, FMN, BH4, etc. and loaded with DAF-2A for 1 h. Potassium solution (50 mM) was used for stimulating varicosities. Fluorescence emission due to DAF-NO adduct was visualized at 515 nm at room temperature. Pharmacological agents were added and equilibrated before DAF loading and stimulation.

Intracellular Recordings

Membrane potentials of antral smooth muscle were measured after impaling with glass microelectrodes pulled on a Sutter instrument (1.2-mm outer diameter, FHC, Brunswick, ME), as described earlier (13). Inhibitory junction potentials were recorded under nonadrenergic noncholinergic (NANC) conditions using the following stimulus settings: 70 V, 1-ms duration square pulses at 20 Hz for 0.5 s. Atropine (1 μM) and guanethidine (5 μM) were added to create NANC conditions. Apamin (0.3 μM) was added to the bath to mask the fast IJP. Stable recordings were obtained from five mice in each group.

Statistics

$P < 0.05$ was accepted as statistically significant after comparison of difference of means using standard parametric methods. For comparison of means between two groups, Student's *t*-test was used.

RESULTS

Enteric Varicosities Stain for PGP9.5

In a given low power field, almost all rounded appearing structures stained for the pan-neuronal marker PGP9.5, thus confirming their neuronal identity (Fig. 1). Varicosities from DBA mice had similar microscopic appearance and staining patterns to that of the WT varicosities.

Colocalization Studies in Varicosities

Myosin Va and nNOSα. Abundant nNOSα staining varicosities were seen in both WT and DBA mice (Fig. 2). To specifically examine the colocalization of myosin Va in the inhibitory varicosities, WT varicosities labeled with myosin Va were probed for colocalization with the inhibitory neurotransmitter marker nNOSα. In Fig. 2, the merged panel shows a high degree of colocalization of myosin Va with nNOSα. In contrast, because of scant expression of myosin Va in DBA mice, nNOSα was present without association with myosin Va.

Myosin Va and LC8. Figure 3 shows robust colocalization of LC8 with myosin Va in WT varicosities. In WT, LC8 was diffusely distributed within the varicosities, but light microscopic resolution could not determine differential subcellular distribution of LC8. DBA varicosities showed similar distributions of LC8 within the core of the varicosity. Due to paucity of expression of myosin Va in DBA varicosities, no colocalization of myosin Va and LC8 was seen.

nNOS and LC8. Figure 4 shows robust colocalization of LC8 with nNOS probed by a COOH-terminal-specific antibody in both WT and DBA varicosities. Thus it is probable that nNOS is transported to the nerve terminals in both WT and DBA mice, where it might associate with LC8 and be stored. In all colocalization studies, care was taken to avoid channel bleed through. Also, one or both primary antibodies were omitted to confirm the specificity of signals (data not shown).

Proximity Ligation Assays to Probe Protein-Protein Interactions In Situ

In situ proximity ligation assay (PLA) was used to examine signals for the following proteins localized at distances of <30–40 nm and indicating possible physical protein-protein interactions (Fig. 5).

Myosin Va with nNOSα. In the WT mice varicosities, fluorescent blobs were visualized using the emission spectra in the red region. These studies indicate close proximity and possible binding of myosin Va to nNOSα. Omission of either primary antibody during PLA assay resulted in the absence of a signal (data not shown). In comparison, these binding signals were not detected in enteric varicosities obtained from DBA mice because of low expression of myosin Va (3.43 ± 0.12 blobs/varicosity in WT vs. none in DBA, mean ± SE, $n = 80$ and

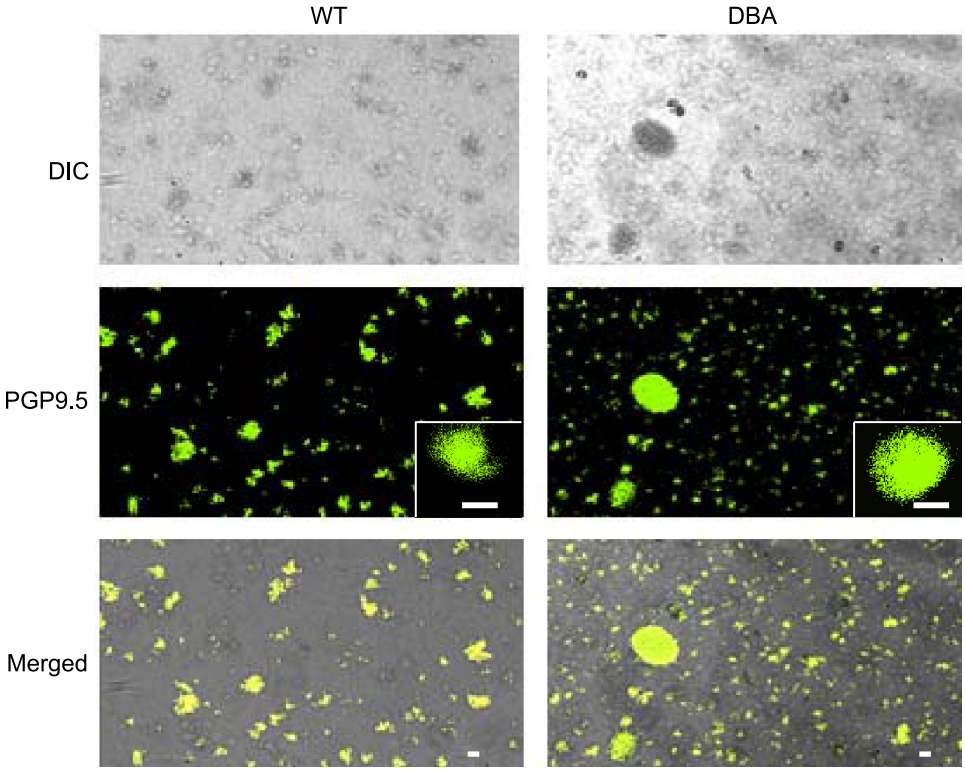

Fig. 1. Enteric nerve varicosities in wild-type (WT) and dilute, brown, non-agouti (DBA) mice. *Top*: light microscopic appearance of the varicosities. Individual varicosities appear rounded in shape. Some plated varicosities form clusters and appear clumped. Varicosities from WT and DBA mice appear similar. *Middle*: PGP 9.5 staining neural structures. *Bottom*: colocalization. Brightness enhancement was applied to whole fields to better visualize fluorescent signals on a transmitted light background. No changes were made to darkness levels, and no nonlinear adjustments were made. Scale bars = 3 μm.

122 WT and DBA varicosities, respectively, from two independent pools, $P < 0.0001$, two-tailed unpaired *t*-test).

Myosin Va with LC8. Figure 5 shows robust binding of LC8 to myosin Va in WT varicosities. Such fluorescent spots of binding were not seen after extensive scans of plated DBA varicosities (7.87 ± 0.25 blobs/varicosity in WT vs. 0.05 ± 0.01 blobs/varicosity in DBA, means ± SE, $n = 90$ and 138 WT and DBA varicosities, respectively, from six independent pools, $P < 0.0001$, two-tailed unpaired *t*-test). These observations are consistent with the fact that LC8 associates with the tail region of myosin Va. Appropriate control experiments were performed to verify the specificity of signals.

nNOS with LC8. Figure 5 shows numerous fluorescent PLA spots of nNOS-LC8 binding in both WT and DBA varicosities (4.11 ± 0.17 blobs/varicosity in WT vs. 3.58 ± 0.22 blobs/varicosity in DBA, means ± SE, $n = 312$ and 90 WT and DBA varicosities, respectively, from six independent pools, $P = 0.12$, not significant, two-tailed unpaired *t*-test). The PLA results suggest that, although nNOS and LC8 are present and remain bound in both WT and DBA varicosities, due to the paucity of myosin Va, LC8-bound nNOS fails to interact with the nerve terminal myosin Va motor in DBA mice.

Lack of Membrane Bound nNOSα in DBA Varicosities

We hypothesized that if myosin Va mediates the transport of nNOS to the plasma membrane, the absence of myosin Va should result in deficiency of membrane-bound nNOSα. Light microscopic examination falls short in determining whether the peripherally located nNOS signal is truly located at the mem-

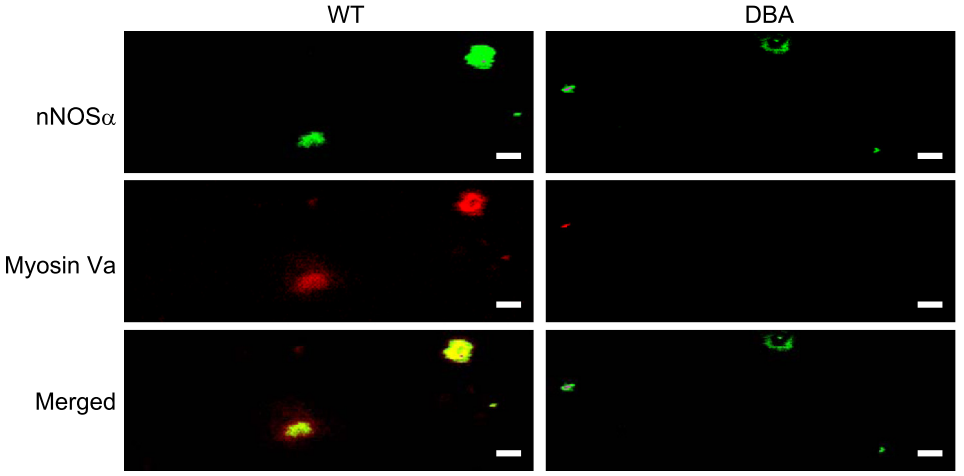

Fig. 2. Myosin Va and neuronal NO synthase (nNOS) α colocalization in WT and DBA varicosities. In WT varicosities, motor protein myosin Va is colocalized with nNOSα, which is diffusely distributed within the varicosity core as well as in a peripheral location with high degree of overlap. In DBA varicosities, signal for myosin Va is markedly reduced or absent. However, nNOSα staining is normal. Note that some myosin Va varicosities did not stain for nNOSα. Slight alteration in pixel saturation was applied to whole fields of images for presentation purpose. Scale bars = 3 μm.

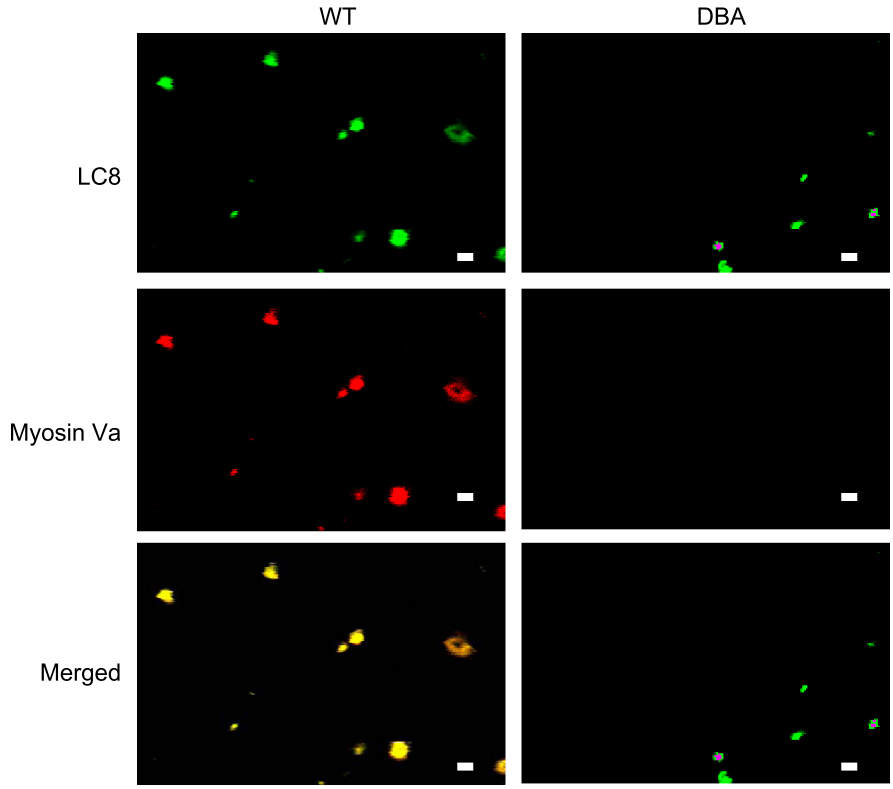

Fig. 3. Myosin Va and LC8 colocalization in WT and DBA varicosities. In WT varicosities, myosin Va and LC8 are colocalized with a high degree of overlap. In DBA varicosities, staining for myosin Va is markedly reduced, but staining for LC8 is normal. Nominal alteration in pixel saturation was applied to these representative images. Scale bars = 3 μm.

brane. We thus separated the membrane and cytosolic fractions of varicosity extracts. An NH_2-terminal-specific nNOSα antibody was used to probe membrane-bound nNOSα transferred to PVDF membranes from polyacrylamide gels. In contrast to WT, membranes of DBA varicosities lacked nNOSα (Fig. 6*A*). Whole varicosities from both WT and DBA mice stained for nNOSα.

In Vitro NO Production in Varicosities

To determine whether myosin Va facilitates NO synthesis during neurotransmission, live imaging of NO production was performed using varicosities loaded with DAF-2DA. K^+-induced stimulation of WT varicosities showed robust NO generation, which was significantly reduced in DBA varicosities (WT, fluorescent DAF-NO signal normalized to area of each varicosity, 55.62 ± 3.05 AU/μm^2 vs. 11.36 ± 0.8 AU/μm^2 in DBA, integrated optical density of green channel estimated on raw images by ImageJ from 46 WT and 36 DBA varicosities, respectively, $n = 6$ pools of varicosities obtained from 30 WT and 18 DBA mice, respectively, $P < 0.0001$, two-tailed, unpaired *t*-test) (Fig. 6*B*). Pharmacological inhibition with L-NAME failed to show the fluorescent DAF-NO signal, whereas addition of NO donor DNO to the bath showed robust intra-varicosity signals (data not shown). These studies suggest that NO production was impaired in DBA mice due to defective membrane localization of active nNOSα.

Smooth Muscle Membrane Potential Studies

Nitrergic (slow) IJP. The WT mice showed compound IJP (inhibitory junction potentials) that consisted of two overlapping components that peaked at 1.0 ± 0.3 and 3.6 ± 0.1 s after onset of the stimulus and represented fast and slow IJPs. The fast and slow components were 18.5 ± 0.3 and 9.1 ± 0.7 mV in WT (25 recordings/5 mice). The fast IJP was masked by apamin (0.3 μM), a small conductance potassium channel inhibitor, revealing only the nitrergic IJP. The nitrergic slow IJP was 9.1 ± 0.7 mV in the WT controls (25 recordings/5 mice) and 3.4 ± 0.3 mV in the DBA mice (11 recordings/5 mice). This decrease in slow IJP in DBA mice was highly significant ($P < 0.0001$) (Fig. 7).

Hyperpolarizing response to NO donor diethylenetriamine-NO. Diethylenetriamine-NO (DNO) (660 μM) produced hyperpolarization of smooth muscle in both WT and DBA mice. The DNO-induced hyperpolarization was 10.7 ± 0.9 mV in the DBA mutants and 9.5 ± 0.8 mV in the control mice (6 recordings/4 mice in each group) (Fig. 7).

DISCUSSION

These studies in isolated enteric varicosities and gastric muscle strips show several things. *1*) In WT mice, the varicosities immunostain for myosin Va and nNOSα with a high degree of overlap. In situ proximity ligation study showed that these two proteins are closely associated. nNOSα was found to be associated with the varicosity membrane and, upon stimulation, these varicosities produced abundant NO. *2*) In DBA mice, the varicosities showed scant staining for myosin Va but normal staining for nNOSα. nNOSα was not found to be associated with varicosity membrane and upon stimulation the varicosities produced little NO. *3*) Electrophysiological studies in antral muscles showed that WT mice had normal nitrergic IJP and postjunctional hyperpolarization responses to the NO donor DNO. On the other hand, DBA mice showed reduced nitrergic IJP but normal hyperpolarization to DNO. Taken together, these results indicate the critical role of myosin Va in

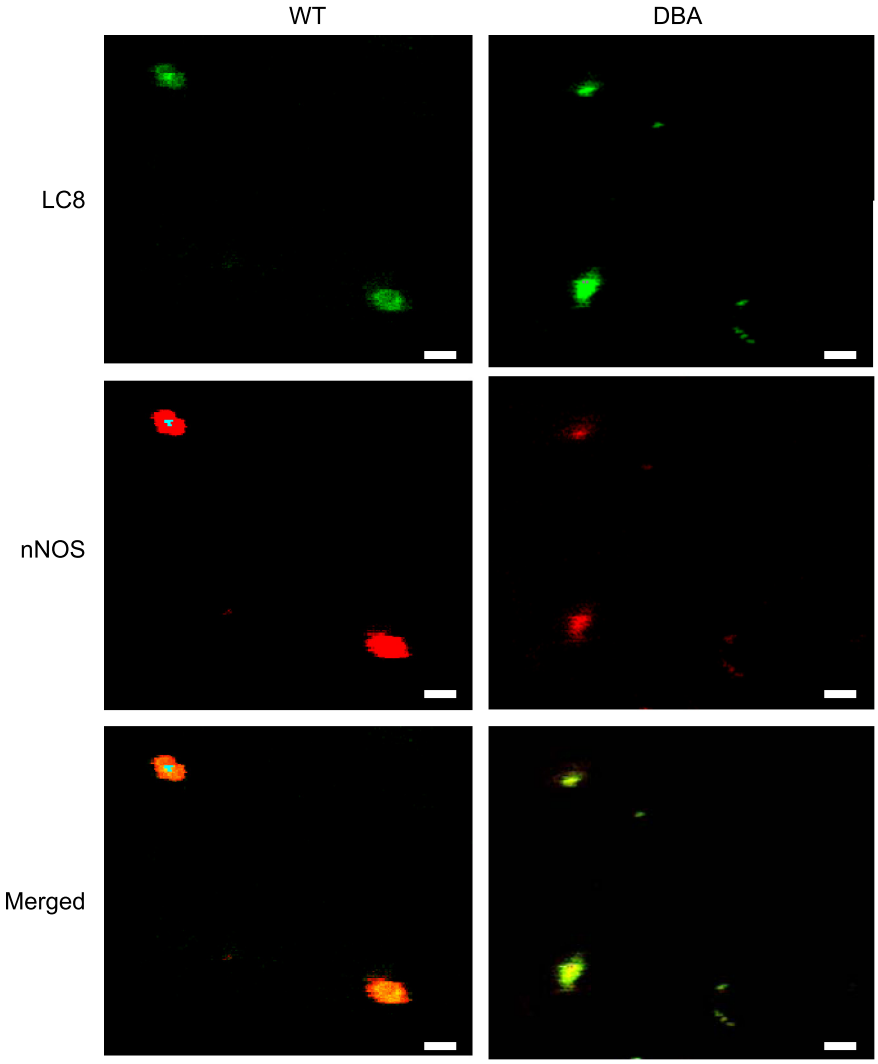

Fig. 4. nNOS and LC8 colocalization in WT and DBA varicosities. In WT as well as in DBA varicosities, LC8 and nNOS were highly colocalized with a high degree of overlap. Nominal alteration in pixel saturation was performed for better visualization of these representative images. Scale bars = 3 μm.

the membrane delivery of nNOS in enteric motor varicosities to impact nitrergic neurotransmission.

Myosin Va is one of three members of the unconventional myosin V subfamily. It takes long 36-nm steps and is a heavy duty, processive motor that takes multiple steps along actin filament without detaching from it (36). Myosin Va is uniquely regulated by cargo binding (16) and is designed for the continuous forward transport of cargo. It is particularly expressed in melanocytes and in a variety of neurons including enteric neurons (28). It has been shown to transport a wide variety of intracellular cargoes (32). However, the role of myosin Va in the transport of nNOS is not known. Using myosin Va-deficient mice, we provide direct evidence that myosin Va translocates the enzyme nNOSα to the varicosity membrane for NO production and release for nitrergic neurotransmission.

Myosin Va has been reported to colocalize with nNOSα in ~28% of enteric neurons (28). The present study demonstrates the colocalization of myosin Va with nNOSα in isolated enteric varicosities. Moreover, in situ proximity ligation assays showed that myosin Va and nNOSα came <40 nm apart from each other, suggesting that they may be physically bound together. These observations support the possibility that myosin Va transports nNOSα within the varicosity. However, the mode of myosin Va binding to nNOSα remains unclear.

We investigated the possibility that LC8 may be the adaptor protein that links myosin Va to nNOSα. We have previously shown that LC8 is localized in the enteric nerve terminals (8). In this study, in situ proximity ligation assays showed that myosin Va and LC8 and LC8 and nNOSα may be bound together. Myosin Va is known to bind cargo at its COOH-terminal tail region (15). The medial tail region of myosin Va is transcribed by six different exons (A–F) (34). These transcripts are alternatively transcribed in a tissue-specific way. Exon B is expressed exclusively in neurons, and exon D is expressed exclusively in melanocytes (34). Molecular cloning has revealed that exon B codon sequence GATGACAAG codes for the three amino acids ^{1284}DDK^{1286} in the tail region of myosin Va (14). This small peptide sequence in myosin Va has been reported to bind to the superficial region of the groove created by the LC8 dimer (29, 38). On the other hand, peptide sequence TGIQVD of nNOSα binds to LC8 in deeper regions of this dimeric groove (19). Thus myosin Va and nNOSα bind to different regions of dimeric LC8. Biophysical modeling studies have also shown that LC8 can simultaneously associate

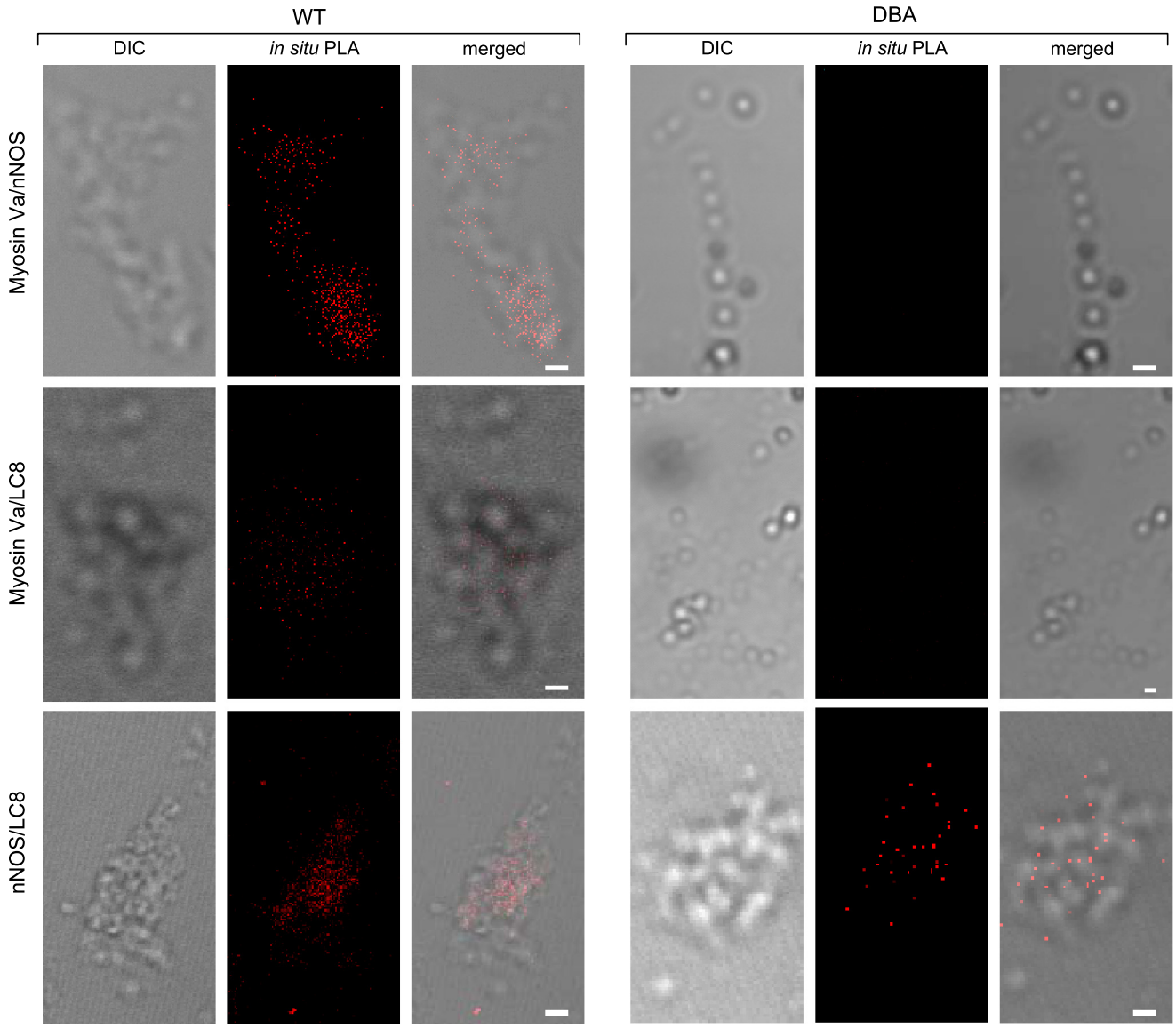

Fig. 5. Proximity ligation in situ assay (PLA) to determine protein-protein proximity. Close proximity is indicated by red fluorescent blobs. *Top*: binding of myosin Va and nNOSα in the cluster of WT varicosities. PLA signals are absent in DBA varicosities because of paucity of myosin Va expression. *Middle*: binding of myosin Va and LC8 in WT varicosities. PLA signals were rarely seen in DBA varicosities. *Bottom*: binding of nNOS and LC8. In both WT and DBA enteric varicosities, PLA signals were seen. Scale bars in all images = 3 μm.

with nNOS and myosin Va (2). These observations suggest that myosin Va may form a tripartite complex with nNOSα via the adapter protein LC8.

It has also been reported that, in the enteric varicosities, nNOSα associates with PSD95 scaffolding protein to tether to membrane (7). In postsynaptic dendrites, nNOS may be transported by myosin Va as a complex macromolecule including myosin Va, LC8, GKAP, PSD95, and nNOSα (24). Guanylate kinase-associated protein (GKAP), similar to nNOSα, has TGIQVD sequences that can bind to deeper regions of the dimeric groove of LC8. Therefore, GKAP may compete with nNOSα for binding to LC8. nNOSα-myosinVa-LC8 may thus form a complex with PSD95, and this synapse-associated, protein-associated protein (SAPAP), GKAP. The exact nature of this proteome in the prejunctional enteric nerve terminals is not known. Further studies are needed to define the relative importance of binding of myosin Va via the adaptor protein LC8 directly with nNOSα or the complex macromolecule involving GKAP and PSD95 in the enteric varicosities. In any case, binding of the nNOSα-containing cargo to the motor protein myosin Va provides an underpinning for transport of nNOSα by myosin Va from interior of the enteric varicosity to the varicosity membrane.

In the enteric varicosities of DBA mice, myosin Va was markedly decreased, but LC8 and nNOS appeared to be normally expressed. Moreover, despite the normal expression of nNOSα, membrane-bound nNOS in the varicosity membrane was markedly reduced, and NO production in response to KCl stimulation in these varicosities was severely impaired. These observations suggested that, in myosin Va deficiency, nNOSα translocation to the varicosity membrane was impaired. Loss of membrane localization was associated with loss of catalytically active nNOSα.

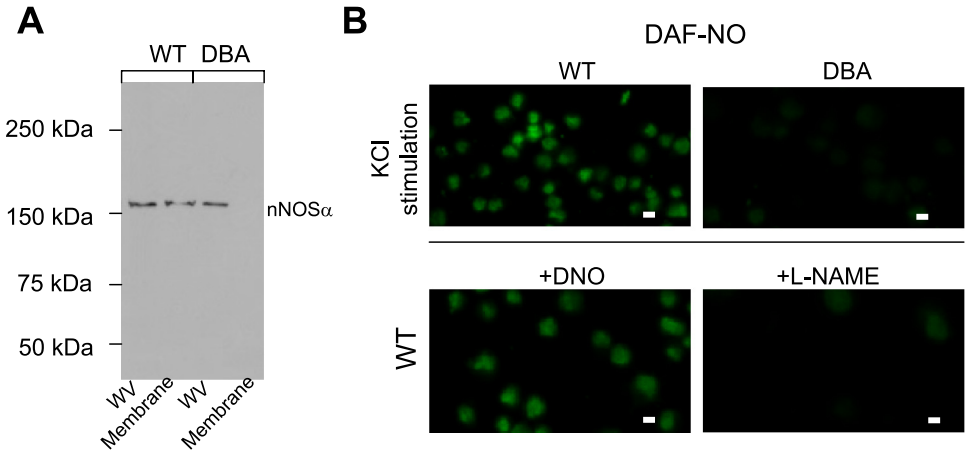

Fig. 6. *A*: Western blot depicting nNOSα in WT and DBA varicosities. Note absence of nNOSα in the lane loaded with membrane extracts from DBA varicosities. Samples were boiled before loading. *B*: in vitro NO production after KCl stimulation in WT and DBA varicosities. Fluorescent NO signal was monitored by preloading the varicosities with the NO indicator DAF-2DA. Note that WT varicosities showed robust NO production after stimulation with 50 mM KCl. In contrast, some DBA varicosities showed only scant DAF-NO signals. Robust signals were seen after preincubation of WT varicosities with DNO. Preincubation of varicosities with L-NAME before KCl stimulation abolished DAF-NO fluorescent signal. Scale bar = 3 μm.

Functional studies of nitrergic inhibitory junction potentials in smooth muscle strips of the gastric antrum further support the role of myosin Va in nitrergic neurotransmission. Nitrergic (slow) IJP was markedly suppressed in myosin Va-deficient DBA mice. The suppression may be due to the decreased NO production and release from nitrergic varicosities or the reduced responsiveness to NO in the postjunctional smooth muscle cells. However, studies of the effect of NO donor (DNO) showed that smooth muscle hyperpolarization to DNO in DBA muscle strips was similar to that in WT strips, suggesting that postjunctional signaling of NO was unimpaired in myosin Va deficiency. These functional observations support the view of reduced NO production and release rather than decreased smooth muscle reactivity in myosin Va deficiency.

Structural abnormalities in the gut in myosin Va-deficient animals have not been examined. Although during our preliminary studies we did not notice any frank morphological abnormalities, more detailed studies of gastrointestinal functions are needed. Electrophysiological studies revealed that, in DBA mice compared with WT controls, there was a 70% reduction in the

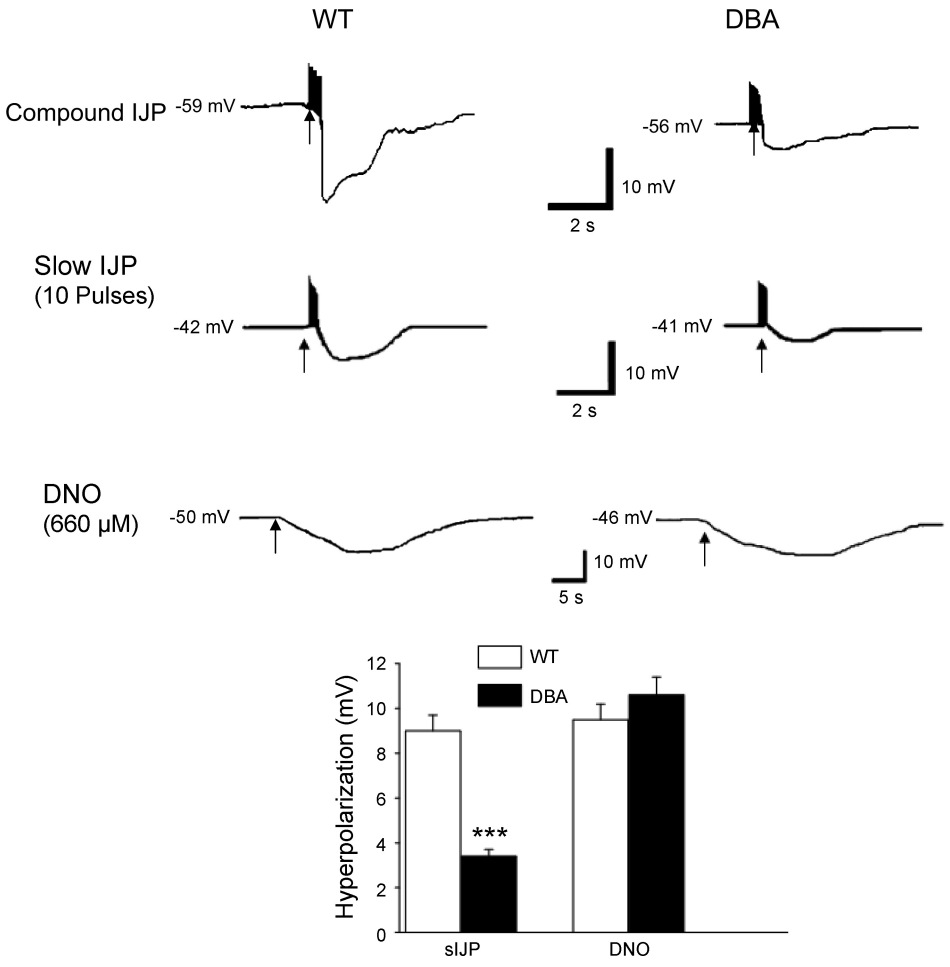

Fig. 7. Nitrergic slow inhibitory junction potentials (sIJP) and smooth muscle hyperpolarization to NO donor DNO in the antral smooth muscle in WT and DBA mice. The upper panel shows examples of compound IJP, middle panel shows slow IJPs, and the bottom panel shows examples of hyperpolarizing responses to NO donor DNO. Histograms show amplitudes of hyperpolarization of the slow IJP and due to DNO. Note that, compared with the WT mice, the nitrergic IJP was markedly reduced in DBA mice. On the other hand, hyperpolarization to DNO was not affected in DBA mice.

nitrergic IJP. This incomplete reduction may be due to the fact that DBA mice have only partial deficiency of myosin Va.

Moreover, our preliminary studies suggest that myosin Va may also be involved in purinergic vesicular transport to the varicosity membrane, and myosin Va deficiency may also cause suppression of purinergic IJP (Chaudhury A, He XD, Goyal RK, unpublished obserations). Myosin Va is not involved in the transport of all types of neurotransmitter vesicles. Selectivity of the neurotransmitter vesicle and transport protein may depend on binding ability of myosin Va to the vesicles. Further studies are needed to determine whether myosin Va transports all types of enteric neurotransmitters and whether its deficiency leads to global loss of enteric neurotransmission.

Deficiency of myosin Va resulted in the loss of nitrergic neurotransmission despite normal nNOSα in the varicosities. This suggests that disorders of nitrergic neurotransmission may not always show changes in expression of nNOSα in the enteric nerves (11, 28). Defective nitrergic neurotransmission accounts for a wide range of gastrointestinal motility disorders (10). Defects in enteric neurotransmission due to the impaired function of intracellular motors may help define the pathophysiology of elusive functional motor disorders of the gut.

In conclusion, these studies show for the first time that myosin Va plays a key role in nitrergic neurotransmission in the enteric nervous system. Myosin Va binds nNOSα via the adapter protein LC8 and translocates it to the varicosity membrane. These studies show the key role that myosin Va plays in the intracellular transport of nNOSα to the varicosity membrane and in nitrergic neurotransmission. nNOS-based nitrergic neuromuscular neurotransmission may be controlled at the transcriptional level (33) or by allosteric modulation (10, 30). The present observations of compartmentalization of active nNOS by precise trafficking in the nerve terminals thereby provide a new level of regulation of nitrergic neurotransmission.

ACKNOWLEDGMENTS

The authors thank Antonietta D'Urso for help in preparation of manuscript.

GRANTS

This work was supported by National Institute of Diabetes and Digestive and Kidney Diseases Grant DK-062867.

DISCLOSURES

No conflicts of interest, financial or otherwise, are declared by the author(s).

REFERENCES

1. **Arundine M, Sanelli T, Ping He B, Strong MJ.** NMDA induces NOS 1 translocation to the cell membrane in NGF-differentiated PC 12 cells. *Brain Res* 976: 149–158, 2003.
2. **Barbar E.** Dynein light chain LC8 is a dimerization hub essential in diverse protein networks. *Biochemistry* 47: 503–508, 2008.
3. **Benashski SE, Harrison A, Patel-King RS, King SM.** Dimerization of the highly conserved light chain shared by dynein and myosin V. *J Biol Chem* 272: 20929–20935, 1997.
4. **Brenman JE, Chao DS, Gee SH, McGee AW, Craven SE, Santillano DR, Wu Z, Huang F, Xia H, Peters MF, Froehner SC, Bredt DS.** Interaction of nitric oxide synthase with the postsynaptic density protein PSD-95 and alpha1-syntrophin mediated by PDZ domains. *Cell* 84: 757–767, 1996.
5. **Brown JR, Stafford P, Langford GM.** Short-range axonal/dendritic transport by myosin-V: a model for vesicle delivery to the synapse. *J Neurobiol* 58: 175–188, 2004.
6. **Bult H, Boeckxstaens GE, Pelckmans PA, Jordaens FH, Van Maercke YM, Herman AG.** Nitric oxide as an inhibitory non-adrenergic non-cholinergic neurotransmitter. *Nature* 345: 346–347, 1990.
7. **Chaudhury A, He XD, Goyal RK.** Role of PSD95 in membrane association and catalytic activity of nNOSalpha in nitrergic varicosities in mice gut. *Am J Physiol Gastrointest Liver Physiol* 297: G806–G813, 2009. Erratum in: *Am J Physiol Gastrointest Liver Physiol* 299: G100–G102, 2010.
8. **Chaudhury A, Rao YM, Goyal RK.** PIN/LC8 is associated with cytosolic but not membrane-bound nNOS in the nitrergic varicosities of mice gut: implications for nitrergic neurotransmission. *Am J Physiol Gastrointest Liver Physiol* 295: G442–G451, 2008.
9. **Espindola FS, Suter DM, Partata LB, Cao T, Wolenski JS, Cheney RE, King SM, Mooseker MS.** The light chain composition of chicken brain myosin-Va: calmodulin, myosin-II essential light chains, and 8-kDa dynein light chain/PIN. *Cell Motil Cytoskeleton* 47: 269–281, 2000.
10. **Gangula PR, Maner WL, Micci MA, Garfield RE, Pasricha PJ.** Diabetes induces sex-dependent changes in neuronal nitric oxide synthase dimerization and function in the rat gastric antrum. *Am J Physiol Gastrointest Liver Physiol* 292: G725–G733, 2007.
11. **Goyal RK, Chaudhury A.** Pathogenesis of achalasia: lessons from mutant mice. *Gastroenterology* 139: 1086–1090, 2010.
12. **Hawkins RD, Son H, Arancio O.** Nitric oxide as a retrograde messenger during long-term potentiation in hippocampus. *Prog Brain Res* 118: 155–172, 1998.
13. **He XD, Goyal RK.** Nitric oxide involvement in the peptide VIP-associated inhibitory junction potential in the guinea-pig ileum. *J Physiol* 461: 485–499, 1993.
14. **Hodi Z, Nemeth AL, Radnai L, Hetenyi C, Schlett K, Bodor A, Perczel A, Nyitray L.** Alternatively spliced exon B of myosin Va is essential for binding the tail-associated light chain shared by dynein. *Biochemistry* 45: 12582–12595, 2006.
15. **Huang JD, Mermall V, Strobel MC, Russell LB, Mooseker MS, Copeland NG, Jenkins NA.** Molecular genetic dissection of mouse unconventional myosin-VA: tail region mutations. *Genetics* 148: 1963–1972, 1998.
16. **Ikebe M.** Regulation of the function of mammalian myosin and its conformational change. *Biochem Biophys Res Commun* 369: 157–164, 2008.
17. **Jenkins NA, Copeland NG, Taylor BA, Lee BK.** Dilute (d) coat colour mutation of DBA/2J mice is associated with the site of integration of an ecotropic MuLV genome. *Nature* 293: 370–374, 1981.
18. **Lajoix AD, Badiou S, Peraldi-Roux S, Chardes T, Dietz S, Aknin C, Tribillac F, Petit P, Gross R.** Protein inhibitor of neuronal nitric oxide synthase (PIN) is a new regulator of glucose-induced insulin secretion. *Diabetes* 55: 3279–3288, 2006.
19. **Lajoix AD, Gross R, Aknin C, Dietz S, Granier C, Laune D.** Cellulose membrane supported peptide arrays for deciphering protein-protein interaction sites: the case of PIN, a protein with multiple natural partners. *Mol Divers* 8: 281–290, 2004.
20. **Leuchowius KJ, Weibrecht I, Soderberg O.** In situ proximity ligation assay for microscopy and flow cytometry. *Curr Protoc Cytom* Chapt 9: Unit 9.36, 2011.
21. **Mabuchi T, Shintani N, Matsumura S, Okuda-Ashitaka E, Hashimoto H, Muratani T, Minami T, Baba A, Ito S.** Pituitary adenylate cyclase-activating polypeptide is required for the development of spinal sensitization and induction of neuropathic pain. *J Neurosci* 24: 7283–7291, 2004.
22. **Mashimo H, He XD, Huang PL, Fishman MC, Goyal RK.** Neuronal constitutive nitric oxide synthase is involved in murine enteric inhibitory neurotransmission. *J Clin Invest* 98: 8–13, 1996.
23. **Mercer JA, Seperack PK, Strobel MC, Copeland NG, Jenkins NA.** Novel myosin heavy chain encoded by murine dilute coat colour locus. *Nature* 349: 709–713, 1991.
24. **Naisbitt S, Valtschanoff J, Allison DW, Sala C, Kim E, Craig AM, Weinberg RJ, Sheng M.** Interaction of the postsynaptic density-95/guanylate kinase domain-associated protein complex with a light chain of myosin-V and dynein. *J Neurosci* 20: 4524–4534, 2000.
25. **Oess S, Icking A, Fulton D, Govers R, Muller-Esterl W.** Subcellular targeting and trafficking of nitric oxide synthases. *Biochem J* 396: 401–409, 2006.
26. **Ohnishi T, Okuda-Ashitaka E, Matsumura S, Katano T, Nishizawa M, Ito S.** Characterization of signaling pathway for the translocation of neuronal nitric oxide synthase to the plasma membrane by PACAP. *J Neurochem* 105: 2271–2285, 2008.
27. **Pastural E, Barrat FJ, Dufourcq-Lagelouse R, Certain S, Sanal O, Jabado N, Seger R, Griscelli C, Fischer A, de Saint Basile G.** Griscelli

disease maps to chromosome 15q21 and is associated with mutations in the myosin-Va gene. *Nat Genet* 16: 289–292, 1997.
28. **Pereira RV, de Miranda-Neto MH, da Silva Souza ID, Zanoni JN.** Vitamin E supplementation in rats with experimental diabetes mellitus: analysis of myosin-V and nNOS immunoreactive myenteric neurons from terminal ileum. *J Mol Histol* 39: 595–603, 2008.
29. **Radnai L, Rapali P, Hodi Z, Suveges D, Molnar T, Kiss B, Becsi B, Erdodi F, Buday L, Kardos J, Kovacs M, Nyitray L.** Affinity, avidity, and kinetics of target sequence binding to LC8 dynein light chain isoforms. *J Biol Chem* 285: 38649–38657, 2010.
30. **Rao YM, Chaudhury A, Goyal RK.** Active and inactive pools of nNOS in the nerve terminals in mouse gut: implications for nitrergic neurotransmission. *Am J Physiol Gastrointest Liver Physiol* 294: G627–G634, 2008.
31. **Rodriguez-Crespo I, Straub W, Gavilanes F, Ortiz de Montellano PR.** Binding of dynein light chain (PIN) to neuronal nitric oxide synthase in the absence of inhibition. *Arch Biochem Biophys* 359: 297–304, 1998.
32. **Rudolf R, Bittins CM, Gerdes HH.** The role of myosin V in exocytosis and synaptic plasticity. *J Neurochem* 116: 177–191, 2011.
33. **Saur D, Neuhuber WL, Gengenbach B, Huber A, Schusdziarra V, Allescher HD.** Site-specific gene expression of nNOS variants in distinct functional regions of rat gastrointestinal tract. *Am J Physiol Gastrointest Liver Physiol* 282: G349–G358, 2002.
34. **Seperack PK, Mercer JA, Strobel MC, Copeland NG, Jenkins NA.** Retroviral sequences located within an intron of the dilute gene alter dilute expression in a tissue-specific manner. *EMBO J* 14: 2326–2332, 1995.
35. **Thatte HS, He XD, Goyal RK.** Imaging of nitric oxide in nitrergic neuromuscular neurotransmission in the gut. *PLoS One* 4: e4990, 2009.
36. **Trybus KM.** Myosin V from head to tail. *Cell Mol Life Sci* 65: 1378–1389, 2008.
37. **Van Geldre LA, Fraeyman NH, Peeters TL, Timmermans JP, Lefebvre RA.** Further characterisation of particulate neuronal nitric oxide synthase in rat small intestine. *Auton Neurosci* 110: 8–18, 2004.
38. **Wagner W, Fodor E, Ginsburg A, Hammer JA 3rd.** The binding of DYNLL2 to myosin Va requires alternatively spliced exon B and stabilizes a portion of the myosin's coiled-coil domain. *Biochemistry* 45: 11564–11577, 2006.
39. **Zhou L, Zhu DY.** Neuronal nitric oxide synthase: structure, subcellular localization, regulation, and clinical implications. *Nitric Oxide* 20: 223–230, 2009.